THE SCRIT ELECTRON SCATTERING FACILITY PROJECT AT THE RIKEN RI BEAM FACTORY*

T. Ohnishi, A. Enokizono, M. Hara, M. Hori, S. Ichikawa
M. Wakasugi, M. Watanabe

RIKEN Nishina Center for Accelerator-Based Science
Wako, Saitama, 351-0198, Japan

K. Adachi, T. Fujita, T. Hori, K. Kurita, M. Togasaki
N. Uchida, K. Yamada

Department of Physics, Rikkyo University, Ikebukuro, Tokyo, 171-8501, Japan

T. Suda, T. Tamae, K. Tsukada

Research Center for Electron–Photon Science, Tohoku University
Mikamine, Sendai, 982-0826, Japan

(Received January 4, 2018)

The SCRIT electron scattering facility has been constructed at the RIKEN RI Beam Factory. The commissioning experiment was performed and the properties of the ion trapping were studied. The first electron elastic scattering experiment of ^{132}Xe was performed and the charge density distribution was obtained. The achieved luminosity in the experiment was $1.8 \times 10^{27}\,\mathrm{cm}^{-2}\,\mathrm{s}^{-1}$ with a 250 mA electron beam current and the injection of 10^8 ions. The production of unstable nuclei has been started with a new online isotope separator (ISOL) system at the SCRIT facility, and developments of the ISOL system for increasing rates of unstable nuclei are underway. Electron scattering with unstable nuclei will be performed in the near future.

DOI:10.5506/APhysPolB.49.483

1. Introduction

Electron scattering is a powerful tool for studying nuclear structure. Since electrons are structureless particles, there are no ambiguous interac-

* Presented at the XXXV Mazurian Lakes Conference on Physics, Piaski, Poland, September 3–9, 2017.

tions, and thus the electron scattering can probe the entire volume of a nucleus without any serious disturbance [1]. Therefore, electron scattering has been used for many years with stable nuclei, from deuteron to uranium.

Recently, the research on short-lived unstable nuclei is very active and continues to expand [2]. In order to study the nuclear structure of unstable nuclei, various reactions have been applied. However, the electron scattering has not been applied to short-lived unstable nuclei because of the difficulty of forming a target and realizing the required high luminosity. Therefore, the electron scattering on short-lived unstable nuclei has been long awaited to improve the understanding of their structure by providing a direct and model-independent information [1].

The SCRIT (Self-Confined Radioactive isotope Ion Target) method [3] is a novel target-forming technique to overcome the aforementioned difficulties. It uses the ion-trapping phenomenon that is observed in an electron storage ring with residual gases. As a result of an intensive and long-term development, the practicality of the SCRIT method has been demonstrated [4, 5]. Then, the construction of an electron scattering facility for unstable nuclei began at the RIKEN RI Beam Factory in 2009 and the commissioning experiment has been performed [6]. In addition, a new online isotope separator (ISOL) system using the photofission of uranium was also constructed at the SCRIT facility and the RI production has been started since 2013 [7]. Recently, we completed the first experiment of electron elastic scattering on ^{132}Xe and deduced the charge density distribution of this nucleus [8].

In this paper, we introduce the SCRIT electron scattering facility and report on its present status and results.

2. SCRIT facility

The SCRIT electron scattering facility [6] consists of a racetrack microtron (RTM), an electron storage ring (SR2), an electron-beam-driven RI separator for SCRIT (ERIS) [7], and a fringing-RF-field-activated ion beam compressor (FRAC) [9]. The SCRIT system is installed in the straight section of the SR2. A window-frame spectrometer for electron scattering (WiSES) is installed beside the SCRIT system, and there is a luminosity monitoring system (LMon) at the downstream exit of the straight section of the SR2 [10]. The schematic layout of the SCRIT facility is shown in Fig. 1.

Electron beams, accelerated by the RTM to 150 MeV, are injected into SR2. After the accumulation in SR2, electron beams from the RTM irradiate a uranium carbide target at ERIS. In ERIS, RIs are produced in a photofission reaction, and they are extracted and transported to the SCRIT system after the mass separation. Between ERIS and the SCRIT system, the FRAC converts continuous RI beams into pulsed RI beams with an ap-

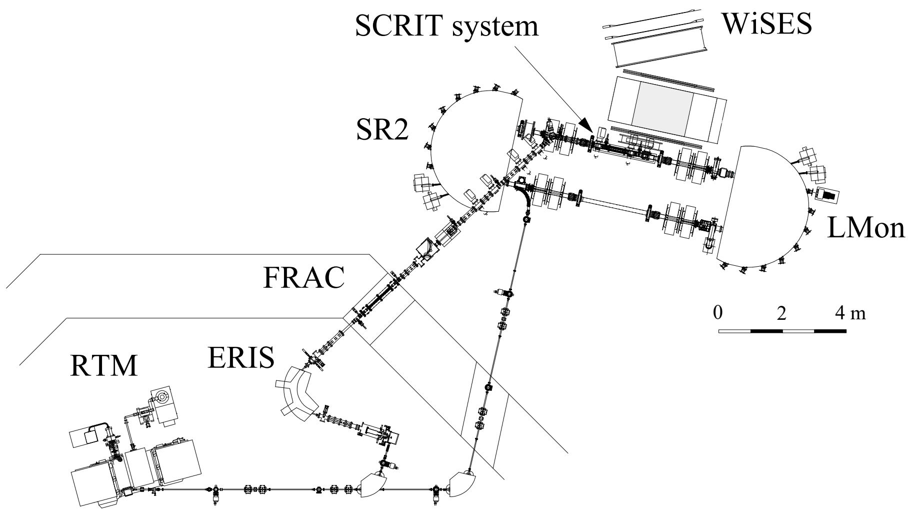

Fig. 1. Schematic drawing of the SCRIT electron scattering facility.

propriate stacking time. The pulsed RI beams are injected into the SCRIT system and trapped. There, electrons that are scattered by trapped ions are momentum-analyzed by WiSES. The luminosity is monitored continuously by the LMon using bremsstrahlung γ rays.

2.1. Accelerators

The RTM is a compact microtron used as an injector for both ERIS and SR2. During injection into SR2, the beam power is approximately 0.4 W with a 2-Hz repetition rate. In the case of RI production, the pulse width of the electron beam is extended from 2 μs to 4 μs, the peak current is 3 mA, and the repetition rate is increased to 10 Hz. This raises the electron beam power to approximately 10 W.

The SR2 is a compact electron storage ring, and the electron beam energy can be varied from 100 to 700 MeV depending on the momentum transfer range required for the experiment. The typical stored beam current and lifetime are 300 mA and 1 Ah, respectively. The size of the electron beam in the SCRIT system is approximately 2 mm and 0.4 mm (σ) in the horizontal and vertical directions, respectively.

2.2. ERIS

RI beams are produced by ERIS, which is an ISOL system that uses photofission of uranium. ERIS consists of a production target, a forced electron beam induced arc discharge (FEBIAD) ion source [11], and a beam-analyzing transport line. Uranium carbide disks of 0.8 mm thickness and 18 mm diameter are used as the production target and heated to around 2000°C for fast effusion and diffusion of the fission products. The produced RIs are ionized in the FEBIAD ion source and accelerated to 6–20 kV. The mass selection is performed in the beam-analyzing transport line. The mass resolution was measured for Xe isotopes and the root-mean-square mass resolution for ^{129}Xe is equal to 1660. A detailed description of ERIS and recent results can be found in Refs. [7, 12].

2.3. FRAC

The FRAC was developed to convert continuous ion beams to pulsed ones under ultra-high vacuum conditions. It is based on the RF quadrupole technique, and consists of six quadrupole electrodes and a set of einzel lens, injection, extraction, and barrier electrodes. The characteristic feature of FRAC is the use of the RF fringing field between the barrier and the quadrupole electrodes. This RF fringing field has both transverse and longitudinal components [13, 14]. Therefore, a fraction of the injected ions can be decelerated in the longitudinal direction without a buffer gas. With the entrance barrier potential lower by a few eV than the kinetic energy of the injected ions, the continuously injected ions are stacked inside FRAC. After the accumulation, they are extracted as a pulse. The pulse width is typically 500 μs and the extraction rate can vary from 1 to 100 Hz.

2.4. SCRIT system

The SCRIT system consists of three electrodes and a switching deflector for ion injection and extraction. The three electrodes are used to form a trap potential in the longitudinal direction; two end electrodes produce the barrier potentials, and the potential applied at the central electrode is set to a few electron volts below the kinetic energy of the injected ions. The electric potential produced by the bunched electron beam is used for the transverse direction trapping.

The ion injection and extraction is controlled by switching the entrance barrier potential. Electrons are scattered automatically in the target region of the SCRIT system. After the trapping time, the trapped ions are extracted and transported to a total charge monitor and an $\vec{E} \times \vec{B}$ velocity filter equipped with channeltrons. There, the total charge and the charge-state distribution of the trapped ions are measured. The measurements with and without the ion injection are performed simultaneously in order to subtract the effect of residual gasses. More details about the SCRIT system can be found in Refs. [6, 15].

2.5. Detector systems

WiSES consists of a window-frame dipole magnet, a pair of long plastic scintillators providing a trigger, and several additional scintillators that help reducing the background. The front (FDC) and rear (RDC) drift chambers are installed at the entrance and the exit of the dipole magnet, respectively. Between the FDC and the RDC, a vinyl bag filled with He gas is inserted in order to minimize the effect of multiple scattering. The trajectories of scattered electrons are reconstructed using the two tracks measured by the FDC and the RDC, with the trajectory calculated using an OPERA-3D field map inside the dipole magnet. One of the characteristic features of WiSES is a wide acceptance using a wide pole gap of the dipole magnet (*i.e.*, 1,700 (w) $\times$290 (h) $\times 1,400$ (d) mm^3). This is to cover the wide trap region of the SCRIT system, which is 500 mm along the electron beam line. In the commissioning experiment [10], the acceptance of the long target region was studied, and the momentum resolution was confirmed to be $\Delta P/P \sim 3 \times 10^{-3}$ at 300 MeV.

LMon is a luminosity monitor that uses bremsstrahlung γ rays. It consists of an array of pure CsI crystals and two fiber scintillator layers. The crystal array consists of seven crystals assembled in a hexagon mesh, and each crystal is a 200-mm-long regular hexagonal cylinder of 40 mm diameter. The two fiber scintillator layers are installed in front of the crystal array in order to measure the horizontal and vertical position distributions. Each fiber scintillator layer consists of sixteen 2-mm-wide fiber scintillators. LMon is located at the exit of the straight section of the SR2, which is 7 m downstream from the SCRIT system. The acceptance and transmission efficiency including the geometrical condition of the SR2 are evaluated by Geant4 simulation.

Detailed description and the performance of the detector system can be found in Ref. [10].

3. Performance of specific elements of the SCRIT facility

3.1. Ion trapping and luminosity properties

The ion trapping properties of the SCRIT system were studied in the commissioning experiment [6, 15]. As a result, it was clarified that the ion trapping features inside the SCRIT system are similar to those of a radio-frequency quadrupole (RFQ) trap because the micro-bunched electron beam creates a periodic potential similar to that of an RF potential. This result explains the trend of the acceptance with mass-to-charge ratio and the ion-trapping lifetime in the SCRIT system. In addition, it was also found that the ion trapping in the SCRIT system is affected by the space-charge effect, the high ionization of trapped ions, the electron beam instability, and other factors. Therefore, there is no stable periodical solution for the ion motion.

The trapping efficiency was obtained from the total charge and the charge state distribution measured by the detector system at SCRIT and it reaches almost 90%. In addition, the number of target ions that participated in the electron scattering on ^{132}Xe was evaluated from the obtained luminosity for a 1-s ion trapping time. The electron beam current and size at the SCRIT system were 175 mA and 3.6 mm^2(σ), respectively. The number of the injected ions was 2.3×10^8 within a 300 μs pulse width. The obtained luminosity was 1.4×10^{27} cm^{-2} s^{-1}. The number of target ions was evaluated as 4.6×10^7 with one pulse injection. The resulting ratio of target ions to those injected was almost 20%. This is due to the large emittance of the injected ions. The ion beam transport is currently being improved.

Figure 2 shows the trapping time evolution of the luminosity measured by LMon under different electron beam conditions. These time evolutions were obtained with different electron beam energy E_e and SR2 tuning parameters. The measurement times for the data presented in Fig. 2 were about one hour at 200 MeV and about four hours at 300 MeV. It is clear that the decay time of the ion trapping can be much increased by properly selecting the the horizontal and vertical tuning parameters and the electron beam energy. In

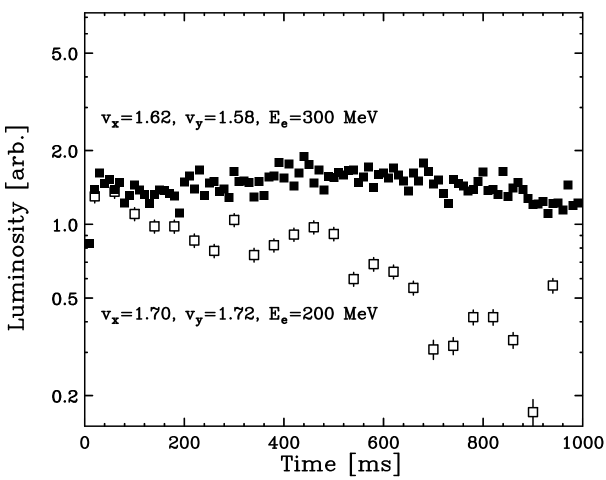

Fig. 2. Trapping-time evolution of luminosity measured using ^{132}Xe ion beams at 6 keV. Luminosity is plotted in arbitrary units. The time evolutions with horizontal and vertical tuning parameters $\nu_x = 1.62$ and $\nu_y = 1.58$, respectively, for the electron-beam energy of 300 MeV (black squares) and with $\nu_x = 1.70$ and $\nu_y = 1.72$ for the energy of 200 MeV (white squares). The error bars represent statistical errors only and, at 300 MeV, they are smaller than the symbols.

addition, the luminosity for $E_e = 300\,\mathrm{MeV}$ increases around 400 ms. This tendency is attributed to increasing of the charge state of trapped ions, which forces the ions into a smaller volume. These results show that the ion trapping can be controlled by adjusting parameters of the electron beam, such as its energy and tuning parameters. After the optimization of electron beam parameters, a luminosity of approximately $1.8 \times 10^{27}\,\mathrm{cm}^{-2}\,\mathrm{s}^{-1}$ was achieved with a 250-mA electron beam and with 10^8 ions per injection.

3.2. RI production at ERIS

We performed the commissioning experiment of the RI production. In total, we prepared 23 uranium carbide target disks [16], and the total amount of uranium used was about 15 g. They were irradiated with the RTM electron beam with a beam power of around 10 W. Tantalum disks with a thickness of 5 mm and a diameter of 20 mm were inserted in front of the production target in order to increase the production of γ rays. The target temperature was kept at approximately 2,000°C. The produced RIs were accelerated to 20 keV and transported for particle identification to a rotating disk, where γ rays related to the beta decay of RIs were measured with a Ge detector. The observed rates for ^{132}Sn and ^{138}Xe were 2.6×10^5 and 3.9×10^6 atoms s^{-1}, respectively. These rates were estimated from the number of observed γ rays based on the efficiency of the Ge detector and the halflife of each isotope. Comparing the obtained rate with the expected production rate inside the target gives the overall efficiency, including the release efficiency from the target, the ionization efficiency inside the ion source, and the transport efficiency of the beam line. The production rates of tin and xenon isotopes are estimated using the calculated total production rate of fission products and the independent chain yield [17, 18]. The total production rate of fission products is estimated using the production rate and the energy distribution of gamma rays obtained from a Geant4 Monte Carlo simulation and the measured cross section of the photofission of uranium [19]. The overall efficiencies for ^{132}Sn and ^{138}Xe were found to be 2.1% and 5.5%, respectively. The overall efficiency for stable xenon with a calibrated gas flow was also measured. Since the stable xenon was introduced into the ionization chamber through a gas inlet, the measured overall efficiency for stable Xe includes only ionization and transport efficiency, and is about 15%. In the case of tin isotopes, the same ionization and transport efficiency as that measured for xenon can be assumed [20], which yields the release efficiencies for ^{132}Sn and ^{138}Xe of 14% and 37%, respectively. These results reflect the chemical properties and the halflives of the specific isotopes. In order to increase the release efficiency, improvements of the thermal conditions and the structure of the transfer line between the ion source and the production target are under way.

3.3. Conversion from continuous ion beam to pulsed ion beam at FRAC

We measured the conversion efficiency of FRAC, which is the ratio between the total charge of the extracted pulsed beam to that of the continuously injected beam, and also determined its stacking time dependence. An ion beam of ^{132}Xe at 6 keV was used, and the total charge of the beam was measured using Faraday cups installed at the entrance and exit of FRAC. The beam current of the continuously injected ion beam was about 4.3 nA. Figure 3 shows the stacking time dependence of the conversion efficiency measured at FRAC. The pulse width of the extracted ion beam was 300 μs. For 100 ms stacking time, the conversion efficiency was 2.7% and the pulse height of almost 38.7 nA was achieved, with a 300 μs pulse width.

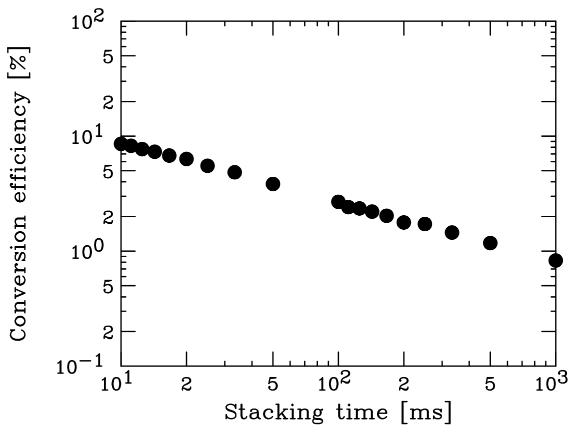

Fig. 3. Stacking time dependence of the conversion efficiency measured at FRAC.

In order to increase the conversion efficiency, various injection schemes (pre-bunching at ERIS, modification of the barrier potential *etc.*) are being developed. This work is still in progress.

4. Results of the first experiment

During the commissioning experiment using ^{132}Xe, its shape was determined precisely with the SCRIT system [8]. Although ^{132}Xe is a stable nucleus, only its root-mean-square charge radius has been obtained in an X-ray measurement of muonic atoms [21]. The commissioning experiment represented thus the first measurement of electron scattering on ^{132}Xe. The electron beam energy was set to 151 MeV, 201 MeV, and 301 MeV, in order to cover a wide momentum transfer region. The number of ^{132}Xe ions was around 10^8. The trapping time was 240 ms and the measurements with and without target ions were performed in order to estimate the background contribution. The typical beam current ranged from 250 mA to 150 mA.

Figure 4 shows the obtained momentum transfer distributions. The systematic error was estimated as 5%, and is mainly due to the ambiguity in the spectrometer acceptance. As a result of the comparison with a phase shift calculation [22] assuming a 2-parameter Fermi density distribution, the charge density distribution of ^{132}Xe nucleus was deduced. The values that reproduced the data best were $c = 5.42^{+0.11}_{-0.08}$ fm and $t = 2.71^{+0.29}_{-0.38}$ fm. The root-mean-square charge radius was calculated as $\langle r^2 \rangle^{1/2} = 4.79^{+0.12}_{-0.10}$ fm, which is consistent with the value $\langle r^2 \rangle^{1/2} = 4.787$ fm obtained in an X-ray measurement of muonic atoms [21]. This result demonstrates that the SCRIT technique enables us to perform elastic electron scattering in order to determine the nuclear charge density distribution, even for a relatively small number of atoms of rare isotopes.

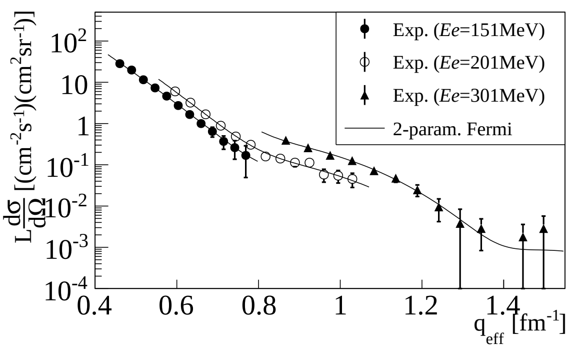

Fig. 4. Momentum transfer distribution of acceptance-corrected yields for ^{132}Xe. The solid line shows a phase shift calculation assuming the nuclear charge density distribution obtained using a 2-parameter Fermi distribution.

5. Future plan

For the first experiment with short-lived unstable nuclei, the electron beam power at RTM will be upgraded from 10 W to 50 W by increasing the beam current of electron gun and the repetition rate. Several other improvements are also in progress, such as the optimisation of the ionization and extraction processes at ERIS and the ion optics of the transport and the injection for the SCRIT system. In addition, in order to reduce background events and improve the momentum resolution, a new SCRIT electrode and a new drift chamber will be installed soon. After these improvements, we will perform the first electron scattering experiment with the short-lived ^{138}Xe nuclei. Furthermore, an introduction of high electron beam power of the order of a few kW is planned in order to perform an experiment with ^{132}Sn.

One of the future projects at the SCRIT facility is to measure the total photo-absorption cross section of short-lived nuclei [1]. The inelastic electron scattering measured at forward angles will provide the crucial information on the structure of excited states and on the collective excitation dynamics. For such a forward angle measurement, a new configuration of the electron storage ring and detector system is under investigation.

6. Summary

The SCRIT electron scattering facility has been constructed and the commissioning experiment was performed successfully. The properties of the ion trapping in the SCRIT system were studied and the achieved luminosity is approximately $1.8 \times 10^{27}\,\mathrm{cm}^{-2}\,\mathrm{s}^{-1}$ with a 250 mA electron beam current and the injection of 10^8 ions within a 300 μs pulse width. An electron elastic scattering experiment was performed using stable ^{132}Xe ions and the charge state distribution of ^{132}Xe was deduced in a precise way. The production of RIs has already been started for experiments with short-lived unstable nuclei. The developments aiming at increasing the production rate of RIs are in progress, and electron scattering on short-lived unstable nuclei will be performed in the near future.

REFERENCES

[1] T. Suda, H. Simon, *Prog. Part. Nucl. Phys.* **96**, 1 (2017) and references therein.

[2] T. Nakamura *et al.*, *Prog. Part. Nucl. Phys.* **97**, 53 (2017) and references therein.

[3] M. Wakasugi *et al.*, *Nucl. Instrum. Methods Phys. Res. A* **532**, 216 (2004).

[4] M. Wakasugi *et al.*, *Phys. Rev. Lett.* **100**, 164801 (2008).

[5] T. Suda *et al.*, *Phys. Rev. Lett.* **102**, 102501 (2009).

[6] M. Wakasugi *et al.*, *Nucl. Instrum. Methods Phys. Res. B* **317**, 668 (2013).

[7] T. Ohnishi *et al.*, *Nucl. Instrum. Methods Phys. Res. B* **317**, 357 (2013).

[8] K. Tsukada *et al.*, *Phys. Rev. Lett.* **118**, 262501 (2017).

[9] M. Togasaki *et al.*, Proceedings of HIAT2015, 2015, WEPB25; M. Wakasugi *et al.* to be submitted.

[10] A. Enokizono *et al.*, *PoS* **INPC2016**, 092 (2016).

[11] R. Kirchner *et al.*, *Nucl. Instrum. Methods* **133**, 187 (1976).

[12] T. Ohnishi *et al.*, *RIKEN Accel. Prog. Rep.* **48**, 229 (2015).

[13] K.L. Hunter, B.J. McIntosh, *Int. J. Mass Spectrom. Ion Processes* **87**, 157 (1989).

[14] K.L. Hunter, B.J. McIntosh, *Int. J. Mass Spectrom. Ion Processes* **87**, 165 (1989).

[15] M. Ogawara *et al.*, *Nucl. Instrum. Methods Phys. Res. B* **317**, 674 (2013).

[16] T. Ohnishi *et al.*, *RIKEN Accel. Prog. Rep.* **47**, xiii (2014).

[17] D. De Frenne *et al.*, *Phys. Rev. C* **29**, 1908 (1984).

[18] D. De Frenne *et al.*, in: Nuclear Data for Science and Technology, Proceedings of the International Conference, Antwerp, September 6–10, 1982, p. 748.

[19] M. Giaeri, ENDF/B8 MT-18, NNDC; H. Reis *et al.*, *Phys Rev. C* **29**, 2346 (1984).

[20] R. Kirchner, *Rev. Sci. Instrum.* **67**, 928 (1996).

[21] G. Fricke *et al.*, *At. Data Nucl. Data Tables* **60**, 177 (1995).

[22] J. Friedrich, A Phase-shift Calculation Code for Elastic Electron Scattering (unpublished).